

adjusted to fit experimental evaporation data. The present calculation extends this work to proton evaporation and has given us confidence in the fundamental theory for the evaporation of any nucleon from excited nuclei whose charge and nuclear force distribution are known from other kinds of measurements on nuclei in their ground state. With respect to our long range objective, a very satisfying feature of the proton emission is the enhanced sensitivity of the pro-

ton emission on the potential shape over that of the level density on the potential shape.

The authors are very grateful to Professor Donald A. Norton and the Davis Computer Center in general for the seemingly infinite time made available on the IBM-1620 computer required for computing the electrostatic barrier transmission. The authors are also indebted to Professor Wm. W. True for his interest and support of this work.

PHYSICAL REVIEW

VOLUME 140, NUMBER 4B

22 NOVEMBER 1965

Nuclear Size Determination by Neutral-Pion Photoproduction

ROALD A. SCHRACK

National Bureau of Standards, Washington, D. C.

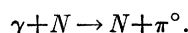
(Received 18 March 1965)

The angular distributions of neutral pions produced by 166-MeV bremsstrahlung on Li, Be, C, O, Mg, Al, Si, S, Ca, and Cu have been obtained by coincident detection of the pion decay photons. The density distributions of nuclear matter have been inferred from the experimental data by means of a Monte Carlo synthesis based on an impulse-approximation elastic-coherent-production model.

INTRODUCTION

THIS paper presents the results of a recently completed set of experiments and their analysis. In a previous paper by Schrack, Leiss, and Penner (SLP) the technique of pion photoproduction as a means of nuclear size determination was investigated using the complex nuclei C, Al, Cu, Cd, and Pb.¹ The results presented in that paper were in general agreement with the results obtained by electron scattering. This set of measurements was initiated to improve and extend the technique and to try to resolve some of the questions that arose as a result of the first series of measurements.

The general layout and experimental method used in this experiment is essentially the same as that used in SLP. A bremsstrahlung beam of peak energy 166 MeV, obtained from the NBS electron synchrotron, was used to photoproduce neutral pions from a variety of complex nuclei (N):



The decay photons from the neutral pions were detected in coincidence in a set of counters designed to provide good determination of the colatitude angle of the pions. Modifications of the equipment from the SLP setup were:

(1) The counter system was altered to improve the shape of the angular sensitivity of the counters to the incident photons. This was done to allow better analytic

representation of the counter in the Monte Carlo synthesis used to analyze the data.

(2) The x-ray beam and target were placed in a vacuum pipe to reduce backgrounds.

(3) Mechanical stability of the system was improved to permit more precise target and counter placement.

(4) Shielding and collimation were improved.

In addition, the analysis was refined to include the effects of the electron pulse shape of the synchrotron, x-ray beam alignment, target size, and counter angular-sensitivity shape. A more complete description of the experimental and analytical technique is given elsewhere.^{1,2}

THEORY

The angular distribution of neutral pions obtained by photoproduction from complex nuclei has been explained on the basis of an elastic coherent model in which the spin-independent part of the interaction plays the only important role.¹⁻³ Under these assumptions the cross section in the center-of-mass system for production of pions of momentum k at angle θ is

$$\sigma(k, \theta) = A^2 F^2(q) (\sin^2 \theta) \sigma_p(k),$$

where A is the mass number of the nucleus, $\sigma_p(k)$ is the spin-independent pion photoproduction cross section from hydrogen, and $F(q)$ is the elastic form factor of the

¹ R. A. Schrack, J. E. Leiss, and S. Penner, Phys. Rev. **127**, 1772 (1962).

² R. A. Schrack, Ph.D. thesis, University of Maryland, 1960 (unpublished).

³ J. E. Leiss and R. A. Schrack, Rev. Mod. Phys. **30**, 456 (1958).

nucleus. $F(q)$ is given by

$$F(q) = \int \rho(r) e^{-i\mathbf{q}\cdot\mathbf{r}} d^3r,$$

where q is the momentum transfer to the nucleus and $\rho(r)$ is the density distribution of the nucleus. While the earlier papers indicated that this model provided an adequate basis for the analysis of the experimental results, at least for the lighter nuclei having spin zero, a special effort was made in the presently reported set of measurements to try to resolve some questions that arose in the analysis of the data of the first paper. In an attempt to determine the presence of any inelastic pion photoproduction an activation curve was obtained for the carbon target. The experimentally obtained activation curve agreed with the activation curve synthesized by the Monte Carlo computer code. While this does not prove that there was no inelastic production of pions, it does indicate that the detection system was predominantly sensitive to elastic production.

To determine the possible contribution of spin-dependent terms on the cross section, a set of experiments was made with Mg, Al, and Si as targets. If there were an appreciable spin-dependent contribution, it would be expected that it would show up in the angular distribution of Al, which has a spin of $\frac{5}{2}$, in comparison with the angular distributions of Mg and Si, which are composed of predominantly spin-zero isotopes. A spin-dependent contribution would be evidenced by a $\cos^2\theta$ term in the angular distribution of Al, but comparison of the experimentally determined angular distributions from Mg, Al, and Si shows no evidence of any such contribution.

The use of the Fourier transform of the density distribution as a form factor to introduce the effect of the spatial distribution of the interaction is a consequence of the assumption that the incoming and outgoing particles can be represented by plane waves. This Born approximation assumption is probably valid for the light nuclei because of the relatively long mean free path of low-energy pions in the nucleus. There are good indications in this work as well as in SLP that the Born approximation model fails for nuclei with $A \geq 40$ under the conditions of this experiment.

The complex nature of the neutral-pion production and detection make a direct analysis of the data difficult. A Monte Carlo synthesis of the expected experimental angular distribution was therefore generated for various nuclear models and compared to the observed experimental angular distribution. Because the neutral pion photoproduction from hydrogen is not known well enough to introduce it as a constant, the normalization of the fitting of experimental data to synthesis is left as a free parameter in the analysis.⁴ The best shape fit is defined as that model of $\rho(r)$ for which the common χ^2

⁴ The normalization used in this paper is not the same as that used in SLP. Multiply the normalization in SLP by 1.34 to make comparisons to this paper.

test of fit of experiment to synthesis is lowest. If we assume that the pion photoproduction cross section is the same for all nucleons and constant regardless of the presence of nearby nucleons, then the normalization of data to theory should be independent of nuclear size. In fact, the normalizations obtained in the best-shape fits of the eight lightest nuclei (where the Born approximation model produces good fits to the data) can be well represented by a constant with no statistical indication of dependence on nuclear size. In the presentation of the results for each element, the best-fit values of the root-mean-square (rms) radius a of the nucleon distributions are given with and without the inclusion of constant normalization as a criterion of fit. All measures of nuclear size in this paper are in units of 10^{-13} cm.

NUCLEAR MODELS

One can infer the density distribution completely only with complete knowledge of the form factor. Figure 1 shows the portions of the form factor that are determined in this experiment. The form factor may be expanded as a power series in the momentum transfer q : $F(q) = 1 - \frac{1}{6}a^2q^2 + \text{higher moment terms}$. The dashed line of Fig. 1 indicates qualitatively the fraction of $F(q)$

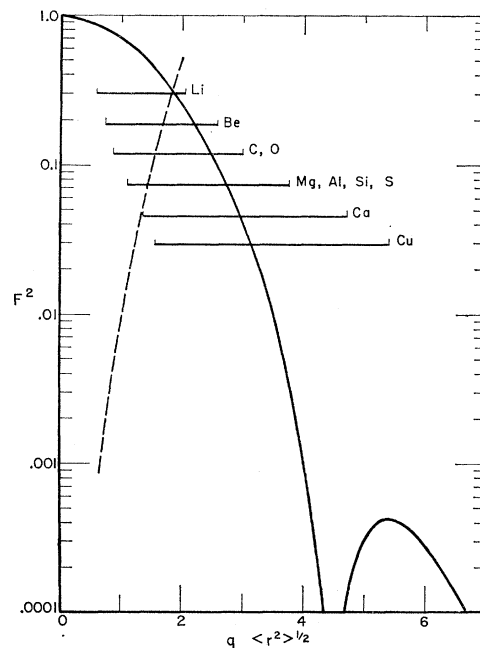


FIG. 1. Range of the form factor measured in this experiment. The solid curve is a representative form factor squared (modified harmonic well with $\alpha=5/3$). The bar labeled by the various elements indicate the approximate span of the form factor curve contributing most heavily to the determination of the angular distributions measured in this experiment. The dashed line is a qualitative indication of the fraction of the value of the form factor contributed by terms not dependent on the rms radius, i.e., $[F - (1 - q^2 \langle r^2 \rangle / 6)] / F$. This function depends on the model used, but the dashed curve represents an upper limit and the value for most models is within 0.6 of the value shown.

that the higher moment terms contribute. Since the contribution of higher moment terms is appreciable even for the lightest nuclei tested, it must be expected that the rms radius of the density distribution inferred from the data will be dependent on the model of the density distribution used.

Because the data of this experiment provide such limited information about the form factor and thus cannot completely determine the density distribution, several models have been used to fit the data. Models have been chosen that have been widely used in the data reduction for other techniques of nuclear size determination, and some effort has been made to compare the results obtained in this experiment and results obtained by other techniques.

This experiment measures the distribution of nuclear matter, both neutrons and protons. Some techniques measure only the charge distribution. For a spherically symmetrical nucleus in which the protons and neutrons have identical distributions one obtains: $a^2(\text{charge}) = a^2(\text{proton}) + a^2(\text{matter})$, where $a(\text{proton})$ is the rms radius of the charge distribution of a proton ($\sim 0.8 \times 10^{-13}$ cm). The change in half-density radius c and edge thickness t is more complicated, but for $t > 2$ the change induced in t when going from matter to charge distributions is much less than the ability to determine t .

Three models were used to fit the data.

(I) The trapezoidal model:

$$\begin{aligned} \rho(r) &= \rho(0) \quad \text{for } 0 < r < r_1, \\ \rho(r) &= \rho(0) \frac{r_2 - r}{r_2 - r_1} \quad \text{for } r_1 < r < r_2, \quad \text{and} \\ \rho(r) &= 0 \quad \text{for } r > r_2, \quad \text{where } t = 0.8(r_2 - r_1). \end{aligned}$$

(II) The Fermi model:

$$\rho(r) = \frac{\rho(0)}{1 + \exp[(r - c)/Z]}.$$

(III) The modified harmonic-well model:

$$\rho(r) = \rho_0 \left(1 + \frac{\alpha k^2 r^2}{a^2} \right) \exp\left(-\frac{k^2 r^2}{a^2} \right),$$

where

$$k^2 = 3(2 + 5\alpha)/2(2 + 3\alpha).$$

The edge-thickness parameter t is defined geometrically as the change in radius obtained when the density changes from 90 to 10% of the central density. The parameter is usually defined for the Fermi model by the relationship

$$t = 4.4Z.$$

The above relationship is valid only as a measure of the density change for the Fermi model when $Z/c \ll 1$. The values of the parameter t given in the description of the nuclear density distributions in this paper should

be thought of as a model parameter only in the algebraic sense for the light nuclei. When $t/c \geq 1.0$ the geometrical value of t may be as much as 20% less than the algebraic parameter.⁵ While the shape parameter t has approximately the same significance for the trapezoidal and Fermi models, the shape parameter α for the harmonic-well model has a different significance. For $4 < A \leq 16$ the parameter α is theoretically related to the number of nucleons in the p shell of the nucleus: $\alpha = \frac{1}{6}(A - 4)$. In the fitting programs the range $0 \leq \alpha \leq 2$ was used whenever a fit to the harmonic-well model was attempted.

The value of α has only a minor effect upon the edge thickness, having its greatest effect upon the density near the center of the nucleus. As a consequence, the modified harmonic well has a limited usefulness as a general data-fitting model and was included for comparison purposes only.

Models I and III are given, respectively, as models XXI and XI in a table of models and their form factors by Hermann and Hofstadter.⁶ The form factor for the Fermi model seems less well known and is reproduced here⁶:

$$\begin{aligned} F_{II}(q) &= \frac{4\pi^2 \rho_0 a^3}{(qa)^2 \sinh^2(\pi qa)} \\ &\times [\pi qa \cosh(\pi qa) \sin(qc) \\ &\quad - qc \cos(qc) \sinh(\pi qa)] \\ &\quad + 8\pi \rho_0 a^3 \sum_{n=1}^{\infty} (-1)^{n-1} \frac{n \exp(-nc/a)}{[n^2 + (qa)^2]^2}. \end{aligned}$$

Since the limited information in the data permits almost equally good fitting by a large number of different forms of even the same model, the only way a complete analysis of the data can be presented is by producing a mapping of goodness of fit of the model to the data as a function of the model parameters. Figure 2 shows such a mapping for the carbon data, using the Fermi model. The shaded area shows the region of statistically acceptable fits. Mappings such as this were produced for all the nuclei studied in this paper for the various models. Although results will be presented in this paper only for selected values of the model parameters, it must be remembered that in general only one size parameter is determined in the experiment uniquely. For example, referring to Fig. 2, if one chooses to fit the data for carbon with the Fermi model with $t = 2.0$, then the data specify a value for the rms radius for that shape model only and the data will specify a different rms radius if t is chosen differently. To conserve space only a limited selection of results will be presented. These will be sufficient, however, to compare

⁵ R. Herman and R. Hofstadter, *High Energy Electron Scattering Tables* (Stanford University Press, Stanford, California).

⁶ L. C. Maximon and R. A. Schrack (to be published).

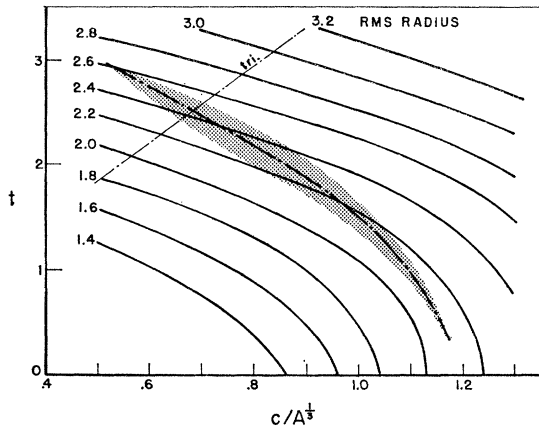


FIG. 2. A mapping of the Fermi model fits for carbon. The shaded area shows the region producing fits within the statistically allowable deviation from the central dashed line which indicates the lowest χ^2 fit. The dashed line marked "tri" indicates the combination of parameters that result in a triangular distribution for the trapezoidal model. Lengths are in units of 10^{-18} cm.

the results of this experiment with the results obtained using other techniques of nuclear size determination.

EXPERIMENTAL RESULTS

Table I shows the results obtained using the Fermi model with t specified and fitting the shape of the angular distribution only, leaving the normalization as a free parameter. Table II shows the results obtained with the Fermi model when constant normalization is imposed as an additional criterion of fit. In the discus-

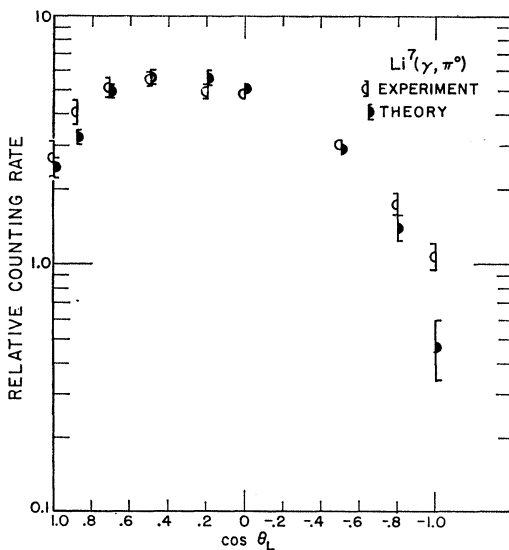


FIG. 3. Experimental data and best-shape fit of the data by the Monte Carlo synthesis for the lithium data. The ordinate is the relative counting rate on a logarithmic plot and the abscissa is the cosine of the colatitude angle of the counter system with respect to the incident x-ray beam. The errors indicated are derived from statistical considerations only. The succeeding figures are labeled in the same manner.

TABLE I. Best-shape fits to the experimental data using the Fermi model and the indicated values of the thickness parameter t . The values given are for the rms radius a and the normalization constant R at the lowest χ^2 obtained for that model. The column labeled N gives the number of data points used in the fitting procedure. In this and succeeding tables all lengths are in units of 10^{-18} cm.

Element	t	a_{II}	R	χ^2	N
Li	1.5	1.64	1.56 ± 0.28	12.0	9
Be	2.0	2.10	1.26 ± 0.21	2.7	8
C	2.5	2.43	1.16 ± 0.08	10.8	10
O	2.5	2.64	1.22 ± 0.29	12.7	9
Mg	2.5	2.95	1.23 ± 0.10	2.7	9
Al	2.5	2.95	1.47 ± 0.19	17.2	9
Si	2.5	3.19	1.03 ± 0.16	10.3	9
S	2.5	3.19	1.29 ± 0.18	23.0	9
Ca	2.5	3.65	0.78 ± 0.22	16.0	8
Cu	2.5	4.17	0.76 ± 0.20	46.0	12

sion which follows only the constant-normalization results for the different models will be given unless otherwise noted. When comparisons are made to results obtained by other experimental techniques, the sizes given will always be for matter distributions.

The experimental results and best shape fit obtained by the Monte Carlo synthesis are shown in Figs. 3 through 12. In these figures the ordinate is the relative counting rate and the abscissa is the cosine of the laboratory colatitude of the counter system (which is approximately the mean laboratory angle of the neutral pions). A complete description of the system and the angular resolution of the counter system to neutral pions is presented in the earlier papers.¹⁻³ It should be noted that the points on the figure representing the results of the Monte Carlo synthesis have statistical errors (indicated by the error flags) of approximately the same magnitude as the experimental data. The Monte Carlo computer code was run only long enough to obtain adequate accuracy, so that the statistical errors on the experimental data were the limiting factor in the accuracy of the analysis. For lithium and beryl-

TABLE II. Best fits of the data using the Fermi model when constant normalization for the eight lightest elements is included as a criterion of fit. The average value of R is determined to be $\bar{R} = 1.22 \pm 0.05$ with a χ^2 of 5 and no statistical indication of R dependence on nuclear size. The last column gives the value of $r_0/A^{1/3}$, where $r_0^2 = (5/3)a^2$.

Element	t	a_{II}	$r_0/A^{1/3}$
Li	2.0	1.98 ± 0.08	1.34 ± 0.05
Be	2.0	2.13 ± 0.08	1.32 ± 0.05
C	2.5	2.39 ± 0.1	1.34 ± 0.05
O	2.5	2.64 ± 0.1	1.35 ± 0.05
Mg	2.5	2.96 ± 0.1	1.32 ± 0.05
Al	2.5	3.09 ± 0.1	1.33 ± 0.05
Si	2.5	3.08 ± 0.1	1.31 ± 0.05
S	2.5	3.23 ± 0.1	1.33 ± 0.05

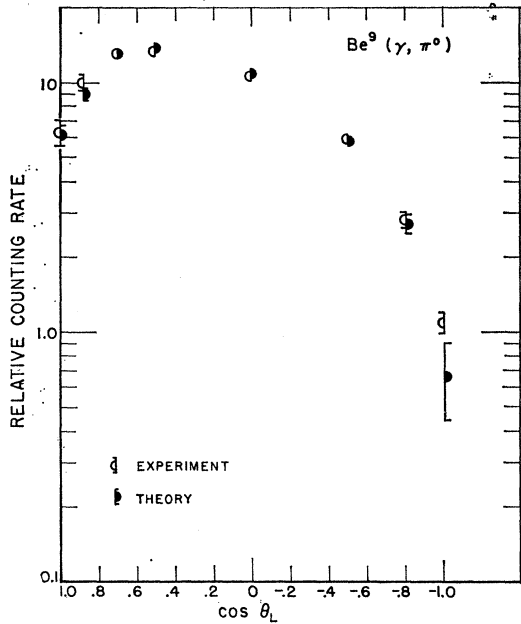


FIG. 4. Experimental data and best-shape fit for beryllium.

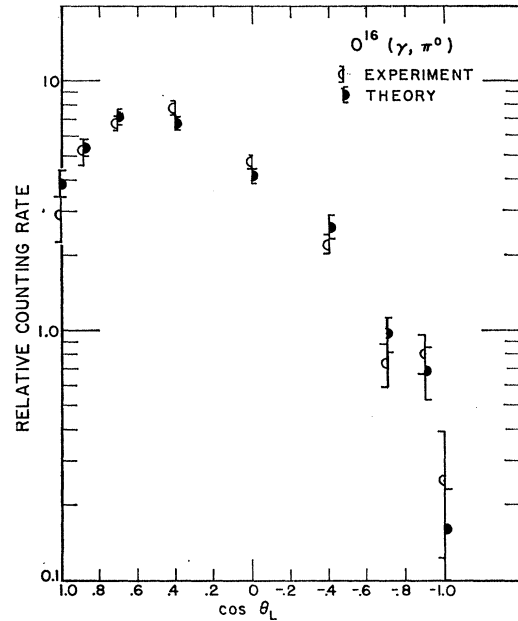


FIG. 6. Experimental data and best-shape fit for oxygen.

lithium the trapezoidal model was not used and for nuclei $A > 16$ the harmonic-well model was not used.

LITHIUM AND BERYLLIUM

The lithium target was approximately 95% Li^7 . The values of the rms radii obtained by the harmonic-well-model fits were independent of the α parameter of the model in the range $0 \leq \alpha \leq 2$, the best fit occurring at

$a_{\text{III}} = 1.93$ for Li and $a_{\text{III}} = 2.12$ for Be. The form factor for the harmonic-well model in the region used to fit the data is very similar to a Fermi model form factor with $t \approx 1.5$. The values obtained for the rms radii with the harmonic-well model thus agree quite well with the results obtained in the fittings using the Fermi model with the value of t . The quality of fit obtained by the Fermi model is weakly dependent on the value of t . For

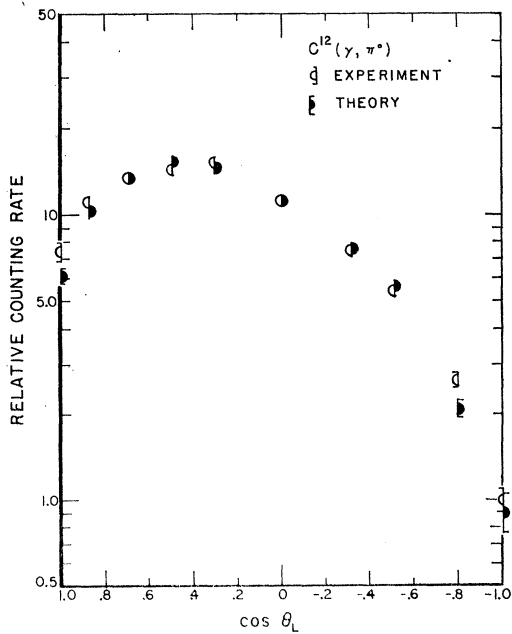


FIG. 5. Experimental data and best-shape fit for carbon.

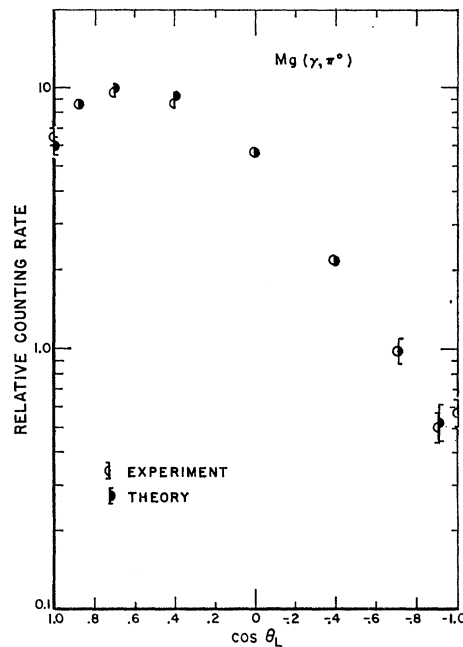


FIG. 7. Experimental data and best-shape fit for magnesium.

example, with lithium the best fit occurs at $t=2.0$ with $a_{II}=1.98 \approx 0.08$,⁷ as indicated in Table II. However, values between $a_{II}=1.88$ at $t=1.0$ and $a_{II}=2.3$ at $t=2.5$ are statistically acceptable fits.

CARBON AND OXYGEN

Carbon and oxygen were the only nuclei fit with all three models. The results for the trapezoidal model are given in Table III. Using the modified harmonic-well

TABLE III. Rms radii obtained from this experiment using the trapezoidal model and constant normalization. The edge thickness t is 2.5 in all cases.

Element	Rms radius
C	2.21 ± 0.1
O	2.49 ± 0.1
Mg	2.82 ± 0.1
Al	2.98 ± 0.1
Si	2.95 ± 0.2
S	3.12 ± 0.1

model, values of $a_{III}=2.22 \approx 0.1$ at $\alpha=1.33$ for carbon and $a_{III}=2.54 \approx 0.1$ at $\alpha=2.0$ for oxygen were obtained. The values given for the various models are the best fits, but the quality of fit was weakly dependent on the shape parameter as indicated in the Fermi fitting diagram for carbon in Fig. 2.

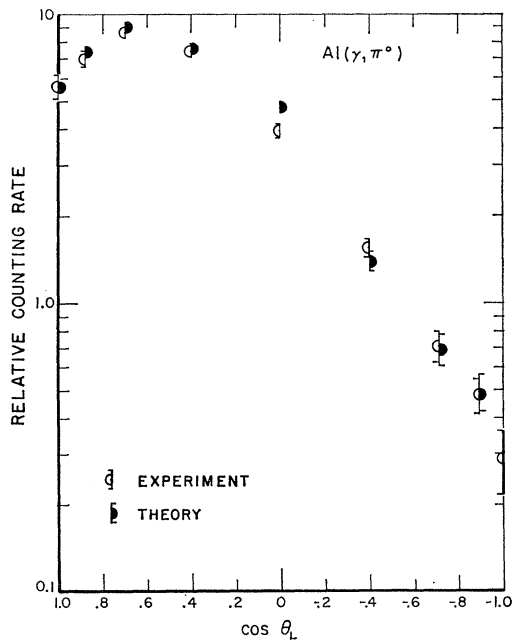


FIG. 8. Experimental data and best-shape fit for aluminum.

⁷ In all expressions of the form $A \pm B$ in this paper, B is the calculated standard deviation of A .

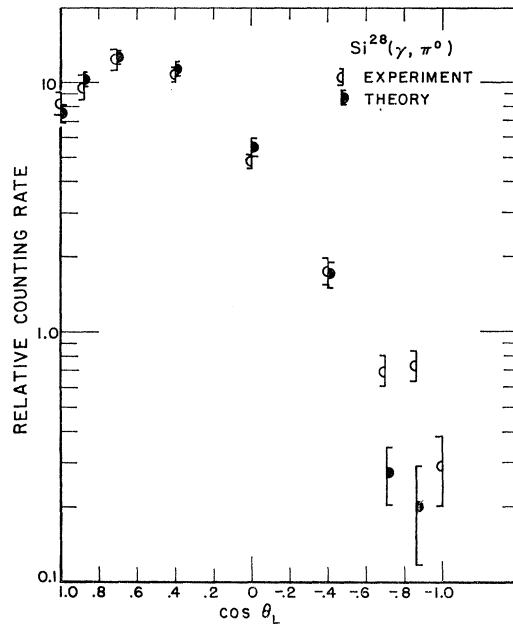


FIG. 9. Experimental data and best-shape fit for silicon.

MAGNESIUM, ALUMINUM, SILICON, AND SULFUR

As discussed earlier, the triad of elements Mg, Al, and Si was investigated to see if any spin-dependent effects could be observed. The data, as shown in Figs. 7, 8, and 9, give no evidence of a spin-dependent contribution to the angular distribution of Al with respect to Mg and Si. The values of the rms radii obtained at $t=2.5$ for Mg, Al, Si, and S using the trapezoidal model

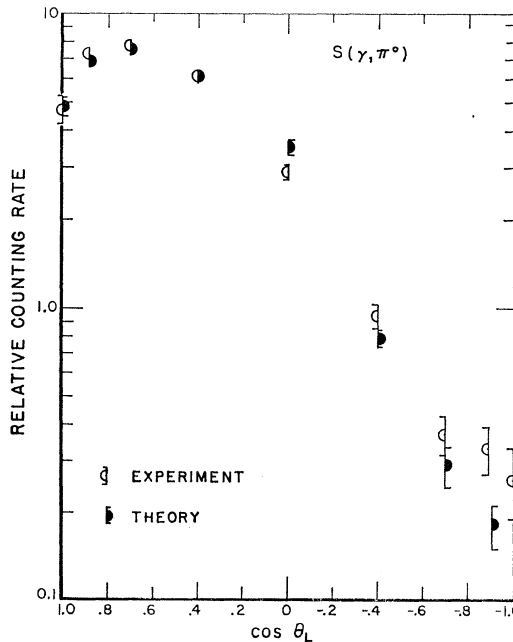


FIG. 10. Experimental data and best-shape fit for sulfur.

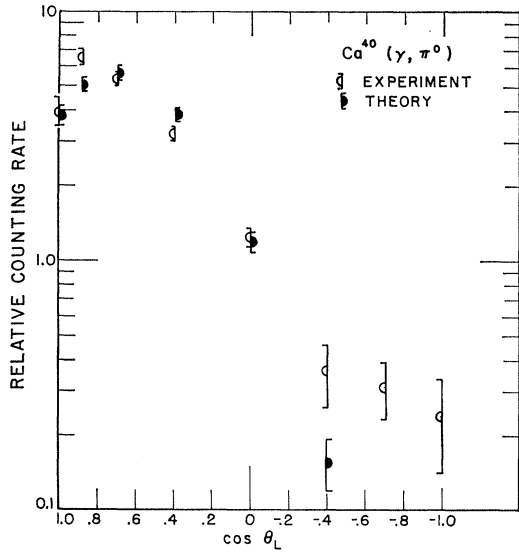


Fig. 11. Experimental data and best-shape fit for calcium.

are given in Table III. Higher errors are given on the Si results because of the difficulty in obtaining a homogeneous target.

CALCIUM AND COPPER

Both the shape of the angular distributions and the normalization obtained with Ca and Cu are not as satisfying as the results obtained with the lighter elements. The difficulty may be understood by reference to Fig. 1. The bar labeled Ca shows the range of momentum transfers that are spanned by the angular distribution of neutral pions produced by 162-MeV photons. The Monte Carlo synthesis indicates that the detection system is designed so that the x rays responsible for producing the detected events have a distribution with a peak at 162 MeV and a full width at half-maximum of about 10 MeV. The angular distribution predicted by the synthesis thus has a very low expected counting rate in the back angles. The experimental data indicate that the cross section is larger than expected in the back angles. It was not felt that a constant normalization assumption should be applied to Ca and Cu. The best shape fit for the Fermi model is given in Table I. The situation for copper is very similar to that of calcium. While the agreement between experiment and theory shown in Fig. 12 is good, the best shape fit shown is for the extreme trapezoidal model with $t=0$ and has an rms radius of $a_T=3.81 \approx 0.12$. The best fit with $t=2.5$ occurs at $a_T=4.17 \approx 0.2$, but the χ^2 of the fit is so high as to make the fit statistically improbable.

The observed counting rates in the back angles for calcium and copper are higher than would be expected using reasonable nuclear density distributions. The excess counting rate in the back angles can be due either to excited state production or to failure of the Born approximation. A failure of the Born approximation seems most probable because it occurs at the first minimum where such failure is generally observed.

COMPARISON OF RESULTS

The results obtained for the rms radii of the density distribution of nuclear matter obtained in this experiment can be compared with values inferred from experiments using other techniques. Table IV shows comparisons made with results obtained from studies of the

TABLE IV. The following table compares values of the rms radius of matter distribution obtained in this experiment with values obtained by other experimental techniques. When the original experimental results indicated the distribution of charge in the nucleus, a matter distribution has been inferred with the assumption that neutrons and protons are similarly distributed. The various experimental techniques referred to are electron scattering (e), neutron scattering (n), negative pion scattering (π^-), and muonic x rays (μ). The models referred to are the Fermi model (II), the modified harmonic-well model (III), the Gaussian-uniform model (GU), and the "family-II" model (F2). The GU and F2 models are similar to the Fermi model. The distribution of Ref. a was obtained from wave functions in a Fermi-shaped well. The distribution thus obtained is similar in shape to the Fermi distribution itself. The parameters of the shape refer to the distribution of matter inferred from the wave functions. The edge thickness is defined in the geometrical sense. The column labeled shape shows the value of the shape parameter used in the model; for III the value of α is given, for the others, the edge thickness parameter t is given. The column labeled π^0 rms shows the value obtained from this experiment for the same model and shape as the comparison experiment. The last column indicates whether the values given for the rms radius given by this experiment and the other experimental technique agree within the sum of the standard deviations of the two experiments.

Element	Reference	Method	Model	Shape	Reference rms	π^0 rms	Agreement
Li ⁷	a	e	II	2.3	2.24	2.10	yes
Li ⁷	b	n	II	2.5	1.85	2.30	no
Li ⁷	c	π^-	II	1.1	1.83	1.88	yes
Be ⁹	d	e	III	0.66	2.12	2.03	yes
Be ⁹	b	n	II	2.5	1.96	2.30	no
C ¹²	e	e	III	1.33	2.29	2.21	yes
C ¹²	b	n	II	2.5	2.21	2.21	yes
C ¹²	c	π^-	II	1.1	2.13	2.11	yes
O ¹⁶	e	e	III	2.0	2.53	2.65	yes
O ¹⁶	b	n	II	2.5	2.50	2.64	yes
Mg ²⁴	f	e	GU	2.6	2.88	3.03	yes
Mg ²⁴	g	μ	F2		3.16	2.97	yes
Al ²⁷	g	μ	F2		3.20	3.11	yes
Si ²⁸	f	e	GU	2.8	2.94	3.18	yes
Si ²⁸	g	μ	F2		3.01	3.13	yes
S ³²	f	e	GU	2.6	3.08	3.23	yes
S ³²	g	μ	F2		2.73	3.23	no
S ³²	h	μ	F2		2.99	3.23	yes
Ca ⁴⁰	i	e	II	2.5	3.43	3.65	yes
Ca ⁴⁰	g	μ	F2		3.16	3.65	no
Ca ⁴⁰	h	μ	F2		3.43	3.65	yes
Cu ⁶⁴	h	μ	F2		3.78	3.81	yes

a L. R. B. Elton and L. A. Swift (private communication).
 b R. Wilson, Nucl. Phys. 16, 318 (1960).
 c W. F. Baker, H. Byfield, and J. Rainwater, Phys. Rev. 112, 1773 (1958).
 d U. Meyer-Berkhout, K. W. Ford, and A. E. S. Green, Ann. Phys. (N.Y.) 8, 119 (1959).
 e H. F. Ehrenberg *et al.* Phys. Rev. 113, 666 (1959).
 f R. H. Helm, Phys. Rev. 104, 1466 (1956).
 g H. L. Anderson, C. S. Johnson, and E. P. Hinks, Phys. Rev. 130, 2468 (1963).
 h D. Quitmann, R. Engfer, U. Hegel, P. Brix, G. Backenstoss, K. Goebel, and B. Stadler, Nucl. Phys. 51, 609 (1964).
 i B. Hahn, D. G. Ravenhall, and R. Hofstadter, Phys. Rev. 101, 1131 (1956); 137, 865 (1965).

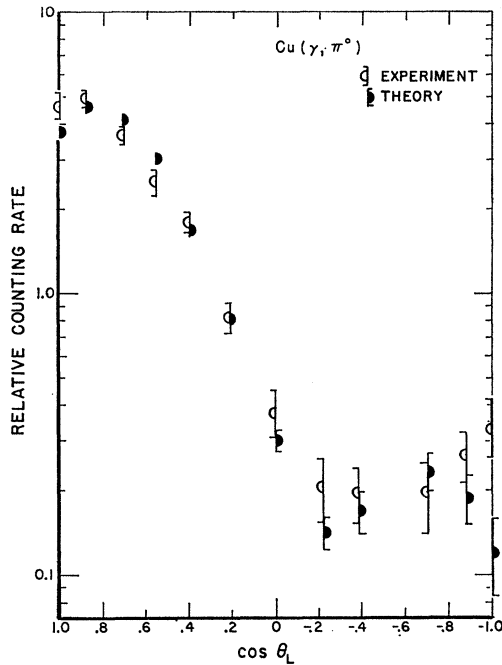


FIG. 12. Experimental data and best-shape fit for copper.

angular distributions for electron scattering, pion scattering, and neutron scattering, and from the energies of muonic x rays. The general agreement seems good.

The ability of the technique to reproduce the data is indicated in Table V, where the results of this experi-

TABLE V. Comparison of rms radii obtained in this experiment and the earlier Schrack-Leiss-Penner (SLP) paper for a trapezoidal model with $t=2.5$ using best shape as criterion of fit.

Element	This experiment	SLP
C	2.14 ± 0.07	2.12 ± 0.14
Al	2.73 ± 0.1	2.74 ± 0.1
Cu	4.05 ± 0.1	3.98 ± 0.2

ment are compared to the results obtained for the same nuclei reported in the earlier SLP paper.

CONCLUSION

Nuclear size determinations from neutral pion photo-production yield values of the rms radius of nuclear matter in generally good agreement with other techniques, but for nuclei with $A > 40$ the model used for the reduction of the data does not appear to be adequate. No spin-dependent contributions are detected when the results obtained from Mg, Al, and Si are compared.

ACKNOWLEDGMENTS

The author is indebted to J. E. Leiss for continued support and to S. Penner and D. Isabelle for their assistance. Special thanks is extended to L. Franklin for his assistance in the taking of data and in various aspects of the analysis. The success of the experimental program was dependent on the skill of the synchrotron operators William Page and Alex Filipovich in producing the required photons.

Low-Lying Levels in ^{50}V and ^{58}Co Studied with the (p,d) Reaction*

J. B. BALL AND R. F. SWEET†

Oak Ridge National Laboratory, Oak Ridge, Tennessee

(Received 12 July 1965)

The low-lying levels in the odd-odd nuclei ^{50}V and ^{58}Co were studied by means of the (p,d) reaction produced with 22-MeV protons from the ORNL 86-inch cyclotron. The deuteron spectra were obtained with a magnetic-spectrograph system having an over-all energy resolution of about 30 keV. The levels observed in ^{50}V are compared with recent calculations on $f_{7/2}$ shell nuclei. The levels observed in ^{58}Co are used to calculate the expected level scheme for ^{56}Co .

I. INTRODUCTION

THE study of levels in odd-odd nuclei is particularly important in attempting to characterize the nature of the nuclear residual interaction as it acts between neutrons and protons. The nature of the residual interaction as it acts between identical particles

is reasonably well established by the large body of experimental data that exists on the energy levels in even-even nuclei. Similar data for odd-odd nuclei are quite scarce.

The characteristic close spacing of levels in odd-odd nuclei requires experimental study with good energy resolution. Since the spins of these levels usually span a rather large range of values, often some levels of interest cannot be populated in decay-scheme-type studies. Except for the very light nuclei, all stable odd-proton nuclei have an even number of neutrons. A

* Research sponsored by the U. S. Atomic Energy Commission under contract with the Union Carbide Corporation.

† Present address: Department of Physics, University of Virginia.